

## RESEARCH LETTER

10.1002/2017GL074706

## Key Points:

- North Indian Ocean sea level has shown significant increase during last three to four decades
- Multidecadal-scale sea level rise in the North Indian Ocean is associated with a weakening of summer monsoon circulation
- Study implies importance of developing policies and adaptation measures to ensure a resilient coastal and regional population

## Supporting Information:

- Supporting Information S1

## Correspondence to:

P. Swapna,  
swapna@tropmet.res.in

## Citation:

Swapna, P., Jyoti, J., Krishnan, R., Sandeep, N., & Griffies, S. M. (2017). Multidecadal weakening of Indian summer monsoon circulation induces an increasing northern Indian Ocean sea level. *Geophysical Research Letters*, 44, 10,560–10,572. <https://doi.org/10.1002/2017GL074706>





Received 24 JUN 2017

Accepted 14 SEP 2017

Accepted article online 19 SEP 2017

Published online 17 OCT 2017

## Multidecadal Weakening of Indian Summer Monsoon Circulation Induces an Increasing Northern Indian Ocean Sea Level

P. Swapna<sup>1</sup> , J. Jyoti<sup>1</sup> , R. Krishnan<sup>1</sup>, N. Sandeep<sup>1</sup> , and S. M. Griffies<sup>2</sup> 
<sup>1</sup>Centre for Climate Change Research, Indian Institute of Tropical Meteorology, Pune, India, <sup>2</sup>NOAA Geophysical Fluid Dynamics Laboratory, Princeton, NJ, USA

**Abstract** North Indian Ocean sea level has shown significant increase during last three to four decades. Analyses of long-term climate data sets and ocean model sensitivity experiments identify a mechanism for multidecadal sea level variability relative to global mean. Our results indicate that North Indian Ocean sea level rise is accompanied by a weakening summer monsoon circulation. Given that Indian Ocean meridional heat transport is primarily regulated by the annual cycle of monsoon winds, weakening of summer monsoon circulation has resulted in reduced upwelling off Arabia and Somalia and decreased southward heat transport, and corresponding increase of heat storage in the North Indian Ocean. These changes in turn lead to increased retention of heat and increased thermosteric sea level rise in the North Indian Ocean, especially in the Arabian Sea. These findings imply that rising North Indian Ocean sea level due to weakening of monsoon circulation demands adaptive strategies to enable a resilient South Asian population.

## 1. Introduction

Sea level rise is emerging as one of the dominant impacts of anthropogenic global warming. It has major societal and geopolitical ramifications for coastal populations and surrounding regions that must absorb populations retreating from inundated coasts. The regions in and around the Indian Ocean are home to roughly 2.6 billion people, which is 40% of the global population. One third of Indian population and the majority of the Asian population are located near coastal regions. Hence, studies of regional Indian Ocean sea level variability and trends are of prime importance to enable suitably planned adaptations to climate change.

Satellite-derived sea level estimates show a rapid increase in North Indian Ocean (north of 5°S) sea level during the last decade (Thompson et al., 2016). Long-term sea level estimates using tide gauge records show a rate of sea level rise of about 1.06–1.75 mm/yr in the Indian Ocean during 1874–2004 (Unnikrishnan & Shankar, 2007; Unnikrishnan et al., 2006) similar to the global sea level rise trend of 1.7 mm/yr estimated for the period 1880–2009 (Church & White, 2011). Though the long-term trend is similar to the global estimates, the sea level in the North Indian Ocean shows multidecadal variability relative to global mean (Figure 1b). There has been significant progress in describing and understanding global sea level rise (Bindoff et al., 2007; Carton et al., 2005; Church et al., 2013; Levitus et al., 2012; Stammer et al., 2013), but the regional departures from this global mean rise are more poorly described and understood (Neil et al., 2014). Unlike global mean sea level rise, North Indian Ocean regional sea level variability is dominated by thermosteric changes (Thompson et al., 2016). The thermosteric sea level rise in the North Indian Ocean is  $0.68 \pm 0.03$  mm/yr during 1958–2015 and has accelerated to  $2.3 \pm 0.09$  mm/yr during 1993–2015 based on ORAS4 reanalysis data. The mechanism contributing to the multidecadal sea level variability in the North Indian Ocean has yet to be described. We here propose a mechanistic hypothesis accounting for multidecadal fluctuations of the North Indian Ocean sea level relative to the global mean.

The decadal and interannual variations of Indian Ocean sea level have received considerable attention. Lee and McPhaden (2008) studied decadal variability in satellite-based sea level in the Indo-Pacific region from 1993 to 2006. Their work was followed by others (Han et al., 2014; Nidheesh et al., 2013; Trenary & Han, 2013). Decadal variability of Indian Ocean sea level was also studied by Unnikrishnan et al. (2006) using tide gauge measurements and Thompson et al. (2016) using satellite-derived sea level data. Though temporal variability of sea level at selected locations or spatial variability for the recent satellite period

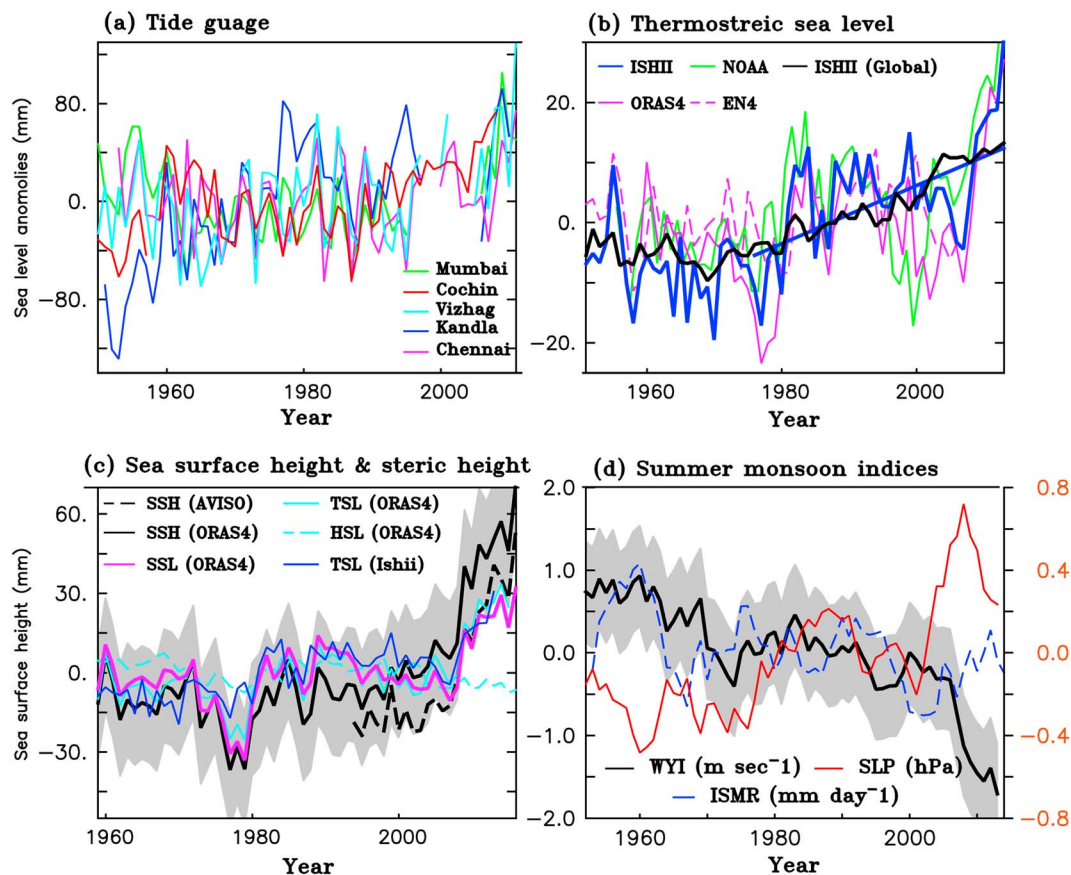


**Figure 1.** Time series of annual mean anomalies of (a) sea level (mm) from tide gauge observations, (b) thermosteric sea level (mm), and (c) sea surface height (SSH), steric height (SSL), thermosteric (TSL), and halosteric (HSL) sea level (mm) in the North Indian Ocean averaged between 50°E–110°E and 5°S–25°N. The trend shown in Figure 1b is for the period 1975–2012 and is significant at 90% confidence level. (d) Time series of anomalies of Webster Yang summer monsoon wind index (WYI, m/s), summer monsoon precipitation (ISMR, mm/d) and sea level pressure (SLP, hPa) over the monsoon trough region (70°E–95°E, 16°N–28°N) during June–September. The error bars based on one standard deviation (shaded) is shown for sea surface height and WY index.

in the Indian Ocean has been studied in detail, long-term multidecadal sea level variability relative to global mean and associated mechanisms remains unknown. The present manuscript offers a new hypothesis for such long-term variability.

The oceans have absorbed over 90% of the excess heat due to anthropogenic greenhouse gas forcing during the past half century (Rhein et al., 2013). This excess heat has caused an increase in the ocean temperature and associated thermosteric sea level rise (Church et al., 2013; Levitus et al., 2012). Another major contributor to the global mean sea level rise is mass addition from melting continental ice. Volume and heat transport into the Indian Ocean from the Pacific Ocean can occur through the Indonesian Throughflow. However, studies have shown that influence of the Pacific anomalies through the Indonesian Throughflow dominates only in the southeast Indian Ocean (Schwarzkopf & Böning, 2011). These results suggest that the thermosteric component of Indian Ocean sea level is the major contributor to sea level variability in the North Indian Ocean, with direct impacts related to redistribution of heat by the Indian Ocean meridional heat transport. This suggestion is further supported by our results.

The novelty of our study is to identify a dynamical mechanism for the regional multidecadal-scale sea level variability in the North Indian Ocean relative to global mean, with a focus on sea level rise measured since 1950. The next section describes the data sets used for the study and the analysis methodology. Section 3 then describes the results, and then discussion and conclusions are presented in section 4.

## 2. Data Sets and Methodology

### 2.1. Observational-Based Measures and Reanalysis Products

The data sets include surface winds and fluxes from the National Centers for Environmental Prediction (NCEP) (Kistler et al., 2001), European Centre for Medium-Range Weather Forecasting (ERA) (Dee et al., 2011), ERA Interim (Berrisford et al., 2011), and the Japanese Meteorological Agency's JRA55 (Kobayashi et al., 2015) reanalysis. The NCEP, JRA55, and ERA Interim are for the period 1950–2016, 1958–2013, and 1979–2015, respectively. The ERA data for the period 1958–1978 merged with ERA Interim are also used for the analysis. Long-term tide gauge records available during the period 1950–2015 are from the archives of Permanent Service for Mean Sea Level (Woodworth & Player, 2003). The upper 700 m thermobaric sea level is calculated from Ishii (Ishii et al., 2003), ORAS4 (Balmaseda et al., 2013), and EN4 (Good et al., 2013) temperature data. We also use the thermobaric sea level anomaly for the upper 700 m from the NOAA/NODC (Levitus et al., 2012). The Ishii and ORAS4 data sets are used for the period 1950–2012 and 1958–2015, respectively, and NODC and EN4 data sets are over the period 1950–2016. Finally, satellite-derived AVISO sea level (<http://marine.copernicus.eu>) and sea surface height (<https://climatedataguide.ucar.edu/climate-data/aviso-satellite-derived-sea-surface-height-above-geoid>) over the period 1993–2015 is used. The climatology is computed for the period 1960–2012 except for AVISO, which is based on years 1993–2015. All the analysis presented in the study is based on annual mean quantities.

### 2.2. Ocean Model and Sensitivity Experiment

We present simulations from a global configuration of the Modular Ocean Model version 4p1 (MOM4p1) Ocean General Circulation Model (OGCM). MOM4p1 is a hydrostatic model configured here using the Boussinesq approximation and a rescaled geopotential vertical coordinate (Griffies et al., 2009). The OGCM is the ocean component of IITM Earth System Model (IITM-ESM) described in Swapna et al. (2014) with simulations well reproducing the mean ocean circulation features (Jadhav et al., 2015; Narayanasetti et al., 2016). Following model spin-up, two idealized experiments are performed using Gill-type wind forcing (Gill, 1980). The chosen wind perturbations broadly mimic the structure of large-scale circulation patterns during a strong summer monsoon circulation (exp1) and a weak summer monsoon circulation (exp2). The strong and weak monsoon conditions are chosen for the experiments to understand the sea level rise from the strong monsoon period prior to the 1970s to the weak monsoon period after the 1970s. Details about the OGCM and wind perturbation experiments are discussed in the supporting information (section S1). In addition, OGCM experiments (exp3 and exp4) are performed by forcing the ocean model with interannually varying wind forcing, keeping all other forcing to climatology. These experiments are performed for the period 1950–2016.

### 2.3. Analysis Methods

#### 2.3.1. Sea Level

The steric, thermobaric, and halobaric sea level are computed over the upper 700 m of the ocean following standard methods, such as detailed in Appendix B of Griffies et al. (2014):

$$\begin{aligned}\eta^{\text{thermobaric}}(\tau) &= \eta(\tau^r) - \frac{1}{\rho_0} \sum dz [\rho(\theta, S^r, p^r) - \rho(\theta^r, S^r, p^r)] \\ \eta^{\text{steric}}(\tau) &= \eta(\tau^r) - \frac{1}{\rho_0} \sum dz [\rho(\theta, S, p^r) - \rho(\theta^r, S^r, p^r)] \\ \eta^{\text{halobaric}}(\tau) &= \eta(\tau^r) - \frac{1}{\rho_0} \sum dz [\rho(\theta^r, S, p^r) - \rho(\theta^r, S^r, p^r)]\end{aligned}\quad (1)$$

where  $\eta^{\text{thermobaric}}(\tau)$  is the thermobaric sea level at time ( $\tau$ ), similarly  $\eta^{\text{steric}}(\tau)$ , and  $\eta^{\text{halobaric}}(\tau)$  are steric and halobaric sea level at time ( $\tau$ ). Variables with an “r” superscript refer to reference state values, so that  $\eta(\tau^r)$  is the sea level at the reference state,  $\rho_0$  is a globally constant Boussinesq reference density,  $\theta$  is the potential temperature of seawater, and  $S$  is the salinity and  $p$  pressure. We choose the upper 700 m as this depth range corresponds to that with the most available observational data. The steric changes in the above equation are described by the sum of  $\eta^{\text{thermobaric}}$  and  $\eta^{\text{halobaric}}$ .

### 2.3.2. Sea Level Budget

$$\Delta\text{SLR}_{\text{Total}} = \Delta\text{SLR}_{\text{Steric}(0-2,000\text{m})} + \Delta\text{SLR}_{\text{Mass}} + R_S \quad (2)$$

where,  $\Delta\text{SLR}_{\text{Total}}$  is the total sea level rise,  $\Delta\text{SLR}_{\text{Steric}}$  is the steric component of sea level in the upper 2000 m, and  $\Delta\text{SLR}_{\text{Mass}}$  is the ocean mass component of sea level. Further details are available in Appendix B of Griffies et al. (2014). The residual is expressed as  $R_S$ , which arises from deep ocean changes.

### 2.3.3. Meridional Heat Transport

The ocean meridional heat transport (MHT) is computed relative to 0°C reference temperature as

$$\text{MHT}(y, t) = \rho_0 C_p \int v \theta dx dz \quad (3)$$

where  $v$  is the meridional ocean velocity,  $C_p = 4185 \text{ J Kg}^{-1} \text{ K}^{-1}$  is the specific heat capacity of seawater, and the reference density is  $\rho_0 = 1025 \text{ Kg m}^{-3}$ .

### 2.3.4. Cross-Equatorial Transport

The strength of cross-equatorial volume transport (CEC) is estimated using the following equation based on Miyama et al. (2003):

$$\text{CEC} = -\frac{1}{\beta \rho_0} \int_{x_w}^{x_e} \frac{\partial \tau^x}{\partial y} dx \quad (4)$$

where  $\tau^x$  is the zonal wind stress at 5° and  $\beta = \frac{\partial f}{\partial y}$ .  $x_e$  and  $x_w$  are the locations of eastern and western boundaries, respectively.  $x_e$  is 110°E, and  $x_w$  is 50°E in the analysis.

## 3. Results

### 3.1. Observational-Based Sea Level Variability in the North Indian Ocean

To help quantify the multidecadal variability of Indian Ocean sea level, we analyze available tide gauge records. Since the data have gaps, we consider only tide gauges with more than 40 years of record during the period 1950–2015. Figure 1a shows time series for annual mean tide gauge sea level anomalies in the North Indian Ocean, revealing a gradual increase since 1950.

Tide gauge observations are available only at selected locations. The broader spatial variability is examined by analyzing the thermosteric sea level using subsurface temperature data in the North Indian Ocean for the region 50°E–110°E and 5°S–25°N. Moreover, in situ ocean temperature and salinity measurements can provide important information about causes of regional sea level change (Levitus et al., 2005) with previous studies pointing to the dominance of thermosteric changes in the North Indian Ocean (Han et al., 2010). We compute annual mean thermosteric sea level anomalies in the upper 700 m in the North Indian Ocean separately using Ishii, ORAS4, and EN4 subsurface temperature data sets (Figure 1b). The time series of thermosteric sea level anomalies shows a multidecadal variability relative to global mean with significant increasing trend during the most recent 40 year period. The trend is computed for the period 1975–2012 and is statistically significant at a 90% confidence level.

To understand the contribution of thermosteric sea level on sea surface height (SSH) in the North Indian Ocean, we analyzed the SSH and steric sea level from AVISO and ORAS4 in the North Indian Ocean. The steric height, thermosteric, and halosteric sea level components are computed using temperature and salinity data from ORAS4 using equation (1) and are shown in Figure 1c. The sea surface height anomalies from ORAS4 shown as the black solid curve in Figure 1c closely follows the steric height anomalies (purple curve). The steric height anomalies are dominated by the thermosteric component (solid light blue curve), with a relatively small halosteric contribution (dashed light blue curve, Figure 1c). The thermosteric anomalies from Ishii (solid blue curve) also follow thermosteric sea level from ORAS4. The anomalies of sea surface height from AVISO (dashed black curve) show the same variability as the thermosteric sea level anomalies from ORAS4 and Ishii for the period 1993–2015. This correspondence suggests that the sea surface height in the Indian Ocean is indeed dominated by the steric height (Salim et al., 2012), with further dominance by the thermosteric component.

We performed a sea level budget analysis to quantify the contribution of thermosteric sea level on North Indian Ocean sea level variability. A sea level budget is estimated based on equation (2) using ORAS4

reanalysis and is shown in Figure S1. The sea level rise in the North Indian Ocean (blue curve) is about  $0.9 \pm 0.04$  mm/yr during 1958–2015, and thermosteric sea level rise (red curve) is  $0.68 \pm 0.03$  mm/yr. Ocean mass changes are estimated based on precipitation minus evaporation and runoff, since mass exchange with Pacific through Indian Ocean Throughflow is confined to the southern Indian Ocean (Schwarzkopf & Böning, 2011). The residual term can be considered as arising due to deep ocean contribution or observational noise. The halosteric contribution is relatively small in the North Indian Ocean (Figure 1c), although accurate estimates of regional halosteric variations warrant improved observations of freshwater fluxes (Liu et al., 2017); we have only considered the thermosteric contribution. The error bounds represent the 95% confidence interval obtained from the least squares fit. It is seen that the sea level rise has accelerated in the recent decades (1993–2015) to about  $3.1 \pm 0.09$  mm/yr, with  $2.3 \pm 0.09$  mm/yr increase in thermosteric sea level. Interestingly, total sea level rise in the North Indian Ocean is comparable with global estimate ( $2.8 \pm 0.02$  mm/yr during 1993–2015 and  $0.96 \pm 0.03$  mm/yr during 1958–2015). The global estimate of thermosteric sea level rise is  $1.3 \pm 0.01$  mm/yr during 1993–2015 and  $0.53 \pm 0.01$  mm/yr during 1958–2015. The total sea level estimates from ORAS4 are comparable with satellite-derived AVISO data during 1993–2015 ( $3.0 \pm 0.18$  mm/yr for the North Indian and  $2.9 \pm 0.04$  mm/yr for global ocean). Therefore, unlike the global mean, which is dominated by additional ocean mass in recent decades (Church et al., 2013), regional sea level variability in the North Indian Ocean is dominated by the thermosteric component which has shown considerable increase during last few decades.

### 3.2. Indian Ocean Sea Level Variability and Variability in Summer Monsoon Circulation

Earlier studies have identified decadal and interannual variability of Indian Ocean sea level (Lee & McPhaden, 2008; Nidheesh et al., 2013; Trenary & Han, 2013). The interannual variability is forced by dominant modes of climate variability such as El Niño–Southern Oscillation (ENSO) and Indian Ocean Dipole (Parekh et al., 2017). Decadal variability in Indian Ocean sea level is predominantly forced by decadal fluctuations of surface wind stress (Li & Han, 2015; Thompson et al., 2016). The previous studies focus on the decadal-scale sea level variability in the Indian Ocean, yet there has to be a mechanism identified for the multidecadal sea level variability.

Variability in ocean and atmospheric circulation can modulate regional sea level variability. The Indian Ocean is land locked to the north, with this geometrical constraint impacting on its meridional heat transport and thermosteric sea level. Furthermore, as shown by Miyama et al. (2003), Indian Ocean meridional volume and heat transport is primarily controlled by the wind stress curl associated with meridional gradients in the zonal wind stress. The annual mean component of the zonal wind stress is predominantly antisymmetric about the equator, with westerlies to the north and easterlies to the south of the equator (Miyama et al., 2003). Likewise, the annual mean wind in the Indian Ocean is dominated by the summer monsoon flow (Schott & McCreary, 2001) with westerlies to the north and easterlies to the south of the equator. Therefore, the meridional ocean heat transport in the Indian Ocean is regulated by the cross-equatorial summer monsoon winds. Correspondingly, multidecadal fluctuations of thermosteric sea level and meridional ocean heat transport in the Indian Ocean are modulated by multidecadal changes in the summer monsoon winds.

The South Asian summer monsoon circulation is characterized by a large-scale cross-equatorial flow that connects the monsoon trough (MT) low-pressure region over the Indian subcontinent in the north and the Mascarene high-pressure region in the southern Indian Ocean (Krishnamurti & Bhalme, 1976). Coherent variations of the South Asian monsoon are known to be consistently reflected in the Webster–Yang monsoon circulation index (WYI), which is a broad-scale circulation measure based on the time mean zonal wind shear between 850 hPa and 200 hPa (U850–U200) averaged over South Asia from the equator to 20°N and from 40°E to 110°E (Webster & Yang, 1992). The time series of the WYI (Figure 1d, black curve) provides evidence for a weakening trend of the summer monsoon circulation. Anomalies of the Webster–Yang summer monsoon wind index and the summer monsoon rainfall (blue curve) show a gradual decrease, while the sea level pressure anomalies (SLP, red curve) during the summer monsoon season over the monsoon trough region (70°E–95°E, 16°N–28°N) show a gradual increase. These results point to a weakening of the large-scale summer monsoon circulation.

The association between multidecadal changes in the winds and weakening of summer monsoon circulation is also evident from the regression analysis of SLP over the MT region on the surface winds during the summer monsoon season (Figure S2d). The regression pattern shows reversal of summer



monsoon cross-equatorial flow and enhanced westerlies over the equatorial Indian Ocean similar to surface wind trend maps from NCEP, ERA, and JRA55 data sets (Figures S2a–S2c). The annual mean wind stress trend pattern is similar to the summer monsoon wind stress trend shown in Figure S2e. The rainfall anomalies during the northeast monsoon or winter monsoon season (October–December) do not show any trend during 1950–2015 (Figure S2f). Thus, the multidecadal surface wind trends over the Indian region are associated with weakening of the summer monsoon. We also present additional support of this relation using OGCM experiments.

The multidecadal changes in winds over the Indian Ocean are dominated by the weakening of summer monsoon circulation. The association between the weakening summer monsoon circulation and sea level rise is investigated by performing a multivariate empirical orthogonal function (MEOF) analysis of thermosteric sea level anomalies and surface wind stress anomalies in the northern Indian Ocean. The global mean sea level is removed from the sea level data to focus on regional variability. To remove interannual and ENSO signals, we apply an 8 year low-pass filter to the anomalies before performing the MEOF analysis. The MEOF pattern is then compared with the spatial pattern of long-term trend in thermosteric sea level anomalies in the North Indian Ocean (Figures 2a and S3a). The long-term thermosteric sea level trend is computed from the Ishii data for the period 1950–2012 and NOAA/NODC data for the period 1955–2015. The sea level anomalies at a 90% confidence level from Mann-Kendall significance test (Kendall, 1975; Mann, 1945) are contoured in Figures 2a and S3a. The spatial pattern of thermosteric sea level anomalies from both Ishii and NOAA show a significant increase in the North Indian Ocean, with higher thermosteric sea level anomalies in the northwestern Arabian Sea in the upwelling regions off Arabia and Somalia, southwest coast of India, east coast of India, and eastern equatorial Indian Ocean. Though there are differences in magnitude of sea level trends between the Ishii and NOAA data, the long-term spatial pattern of thermosteric sea level trend is similar in both data sets. The observed long term sea level trend published by NOAA is shown in Figures S3b and S3c, which is consistent with the thermosteric sea level trend shown in Figures 2a and S3a.

In Figure 2b, we show the leading empirical orthogonal function (EOF) mode (MEOF1) of the North Indian Ocean thermosteric sea level (shaded) and surface wind stress (vectors) variability. The first MEOF mode accounts for 31.8% of the joint variability and is found to be significant based on the methods of North et al. (1982). The dominant sea level signal is a broad-scale rise, especially in the western Arabian Sea off the coasts of Somalia and Arabia, the west coast of India, the Bay of Bengal, and the east equatorial Indian Ocean. This pattern is consistent with spatial trend patterns discussed in Figures 2a and S3a. The MEOF1 spatial structure of the surface wind stress variations shows easterly anomalies to the north of the equator and westerly anomalies along the equator and to the south (Figure 2b) similar to the weakened boreal summer monsoon cross-equatorial flow shown in Figures S2a–S2c. Additionally, during weak monsoon conditions, the westerly flow tends to be oriented along the equatorial Indian Ocean (Krishnan et al., 2006; Ramesh Kumar et al., 2009; Rodwell, 1997; Swapna et al., 2014). The anomalous westerly winds result in thermocline deepening and a rise in sea level in the eastern equatorial Indian Ocean. The time series of coevolution of the North Indian Ocean sea level and wind anomalies are shown by the corresponding first principal component (PC1) from the MEOF analysis (Figure 2c, red curve). PC1 shows a positive trend indicating that the dominant pattern of sea level and wind stress variations (MEOF1) is associated with an upward trend. The upward trend is also seen in the time series of PC1 from MEOF analysis of EN4 sea level and NCEP zonal wind stress anomalies (Figure 2c, green curve). The upward trend in PC1 indicates the coevolution of sea level rise in the North Indian Ocean and wind variations associated with weakening of summer monsoon circulation.

To confirm the relation between the summer monsoon and sea level rise, EOF analysis is performed separately for zonal wind stress over North Indian Ocean and Indian summer monsoon rainfall. The PC1 from the EOF analysis (black and blue curve) are shown along with PC1 from MEOF analysis (red and green curve) in Figure 2c. The association between summer monsoon and sea level is evident from the high correlation between the PC1 of the zonal wind stress (black curve) and sea level (correlation coefficient,  $r = 0.90$ ) and rainfall (blue curve) and sea level ( $r = -0.86$ ). The dominant mode from the EOF analysis of zonal wind stress explains 36.2% and rainfall 33.5% variance, respectively, and is found to be significant based on North et al. (1982). To better understand the dynamics of the North Indian Ocean sea level variability seen in the MEOF analysis, we performed ocean model experiments described in the following section.

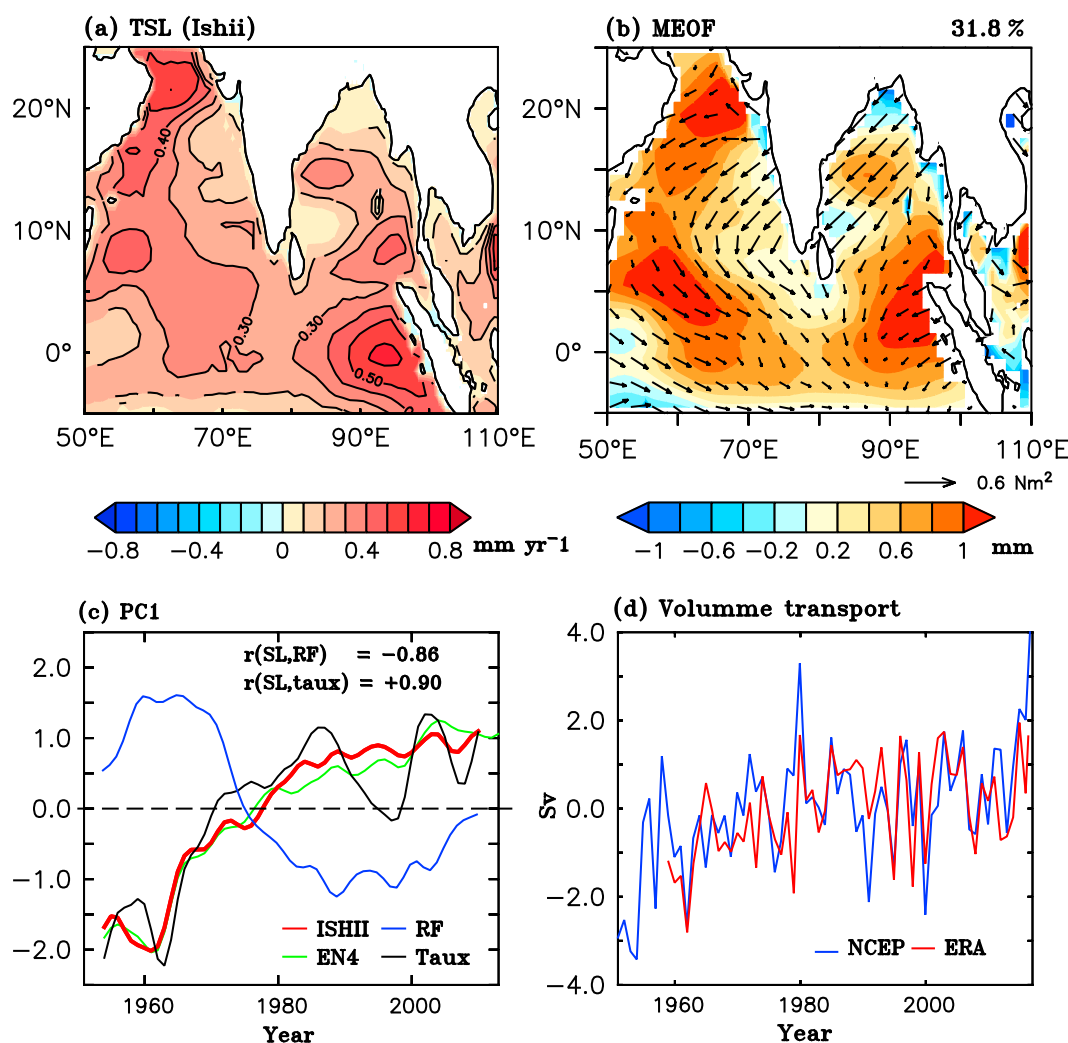


**Figure 2.** (a) Spatial pattern of long-term trend of thermosteric sea level anomalies (mm/yr) in the northern Indian Ocean from Ishii for 1950–2012. (b) Spatial pattern of leading mode of variability from multivariate EOF analysis of 8 year low-pass-filtered thermosteric sea level anomalies (mm, shaded) and wind stress anomalies ( $\text{N m}^{-2}$ , vectors). (c) Time series of first principal component (PC) from MEOF analysis of sea level and NCEP wind stress (red and green curves correspond to Ishii and EN4, respectively). First PC from EOF analysis of summer monsoon rainfall (RF, blue) and zonal wind stress anomalies (taux, black). (d) Time series of meridional volume transport (Sv) at 5° transect based on NCEP (black) and ERA (red) winds. The negative sign indicates southward volume transport.

### 3.3. Dynamics of Multidecadal Sea Level Variability in the North Indian Ocean

Annual mean heat transport in the Indian Ocean is directed southward and is dominated by the summer monsoon circulation (Schott & McCreary, 2001). The Indian Ocean is land locked to the north. Consequently, in a steady state the heat gained in the North Indian Ocean is exported southward across the equator. Studies indicate that the heat is exported through the cross-equatorial shallow overturning cell (Miyama et al., 2003; Schott et al., 2009). The cross-equatorial cell in the Indian Ocean is characterized by shallow meridional overturning circulation with northward flow of Southern Hemisphere thermocline water, upwelling in the Northern Hemisphere, and a return flow of surface water (Miyama et al., 2003). The main driving mechanism for the meridional cross-equatorial ocean heat transport is the summer monsoon, with maximum southward transport during summer monsoon season, leading to annual mean southward heat transports south of the equator (Chirokova & Webster, 2006; Loschnigg & Webster, 2000; Schoenefeldt & Schott, 2006). However, little is known about the role of regional monsoon wind forcing on modulating the multidecadal fluctuations of the meridional ocean heat transport and North Indian Ocean sea level.

### 3.3.1. Implied Meridional Ocean Heat Transport and North Indian Ocean Heat Storage

Long-term measurements of ocean currents are not sufficient to directly compute multidecadal variability of meridional ocean heat transport. As a proxy, we estimate the implied ocean transport from atmospheric reanalysis. To understand the multidecadal variability in heat transport and strength of cross-equatorial cell, we estimated the sverdrup transport, which is primarily contributed by the wind stress curl due to zonal wind stress component (Miyama et al., 2003). Following Miyama et al. (2003) and Thompson et al. (2016), the volume transport is calculated based on equation (4) and the anomalies are shown at the 5° transect from NCEP and ERA data (Figure 2d). The negative sign indicates southward volume transport. As the northern Indian Ocean is located in the tropics, the excessive heat gained in the northern Indian Ocean is transported southward by the southward volume transport. The southward transport from both the data sets shows a gradual decrease, especially after the 1970s similar to the upward trend in PC1 from MEOF analysis (Figure 2c). The annual mean of the cross-equatorial transport in the Indian Ocean is negative. Less negative values indicate a decrease in southward volume transport, which is accompanied by an increase in heat storage and rise in thermosteric sea level in the North Indian Ocean. The upward trend in PC1 from MEOF analysis (Figure 2c) and weakening of southward transport (Figure 2d) can be seen after the 1970s, thus indicating the weakening of summer monsoon circulation and increase in heat storage and rise in thermosteric sea level in the North Indian Ocean.

### 3.3.2. Idealized Wind Perturbation and Sensitivity Experiments With a Numerical Model

To gain further insight on North Indian Ocean sea level response and meridional heat transport changes to weakening monsoonal forcing, we examine two experiments with a global OGCM forced with idealized wind perturbations. Detailed description of Gill-type monsoon wind forcing used in the idealized wind perturbation experiments is discussed in Krishnan and Swapna (2009). The experiment is designed by adding the strong and weak monsoon winds on the climatological winds from CORE (Griffies et al., 2009; Large & Yeager, 2009). One year integration is carried out with each strong monsoon and weak monsoon wind forcing. Details about the wind perturbation experiments are discussed in the supporting information section S1.

The wind stress anomalies used for the sensitivity experiment are shown in Figures S4a and S4b. Weakened summer monsoon circulation features can be inferred from exp2 and stronger circulation features from exp1 (Figure S4a). The zonal variability of wind forcing for exp1 shows enhanced cross-equatorial flow, whereas there is a weakened cross-equatorial flow for the weaker monsoonal winds in exp2 (Figure S4c).

Sea level response from the sensitivity experiments is shown in Figure 3a. The difference in sea level in the North Indian Ocean between exp2 and exp1 reveals sea level rise in the North Indian Ocean in exp2 as compared to exp1. It is interesting to note that sea level rise is more prominently seen in the Arabian Sea than the Bay of Bengal due to the stronger winds in the Arabian Sea. The weakened summer monsoon circulation results in reduced upwelling in the coastal upwelling regions off Somalia and Arabia in the Arabian Sea and the sea level rise is more prominent in these regions. The idealized experiments reveal that changes in the wind pattern over the Indian Ocean have considerable impact on sea level, primarily confined to the Arabian Sea. The simulated patterns of sea level change are consistent with those shown from our analysis of observation-based data in Figure 2.

We compute the annual mean zonal mean (average over 50°E–110°E) ocean meridional heat transport and heat storage from the simulations, with the difference in meridional heat transport between exp2 and exp1 shown in Figure S4d. The meridional heat transport is calculated based on equation (3). Anomalous northward (positive) heat transport during May–October is seen from the exp2 as compared to exp1. The heat transport is southward during May–October and northward during the rest of the season and the annual mean heat transport is dominated by the southward heat transport. The difference map indicates that southward heat transport has decreased during weak monsoon conditions (exp2) as compared to strong monsoon conditions (exp1).

The difference in annual mean zonal mean subsurface temperature (shaded) and cross-equatorial cell (vector) from exp2 and exp1 is shown in Figure 3b. The cross-equatorial cell in the Indian Ocean is characterized by a shallow (less than 500 m) meridional overturning circulation (Miyama et al., 2003). The simulated cross-equatorial cell is represented by meridional and vertical currents (vectors) in Figure 3b. Anomalous weaker cross-equatorial cell and anomalous northward meridional heat transport are seen in exp2 as



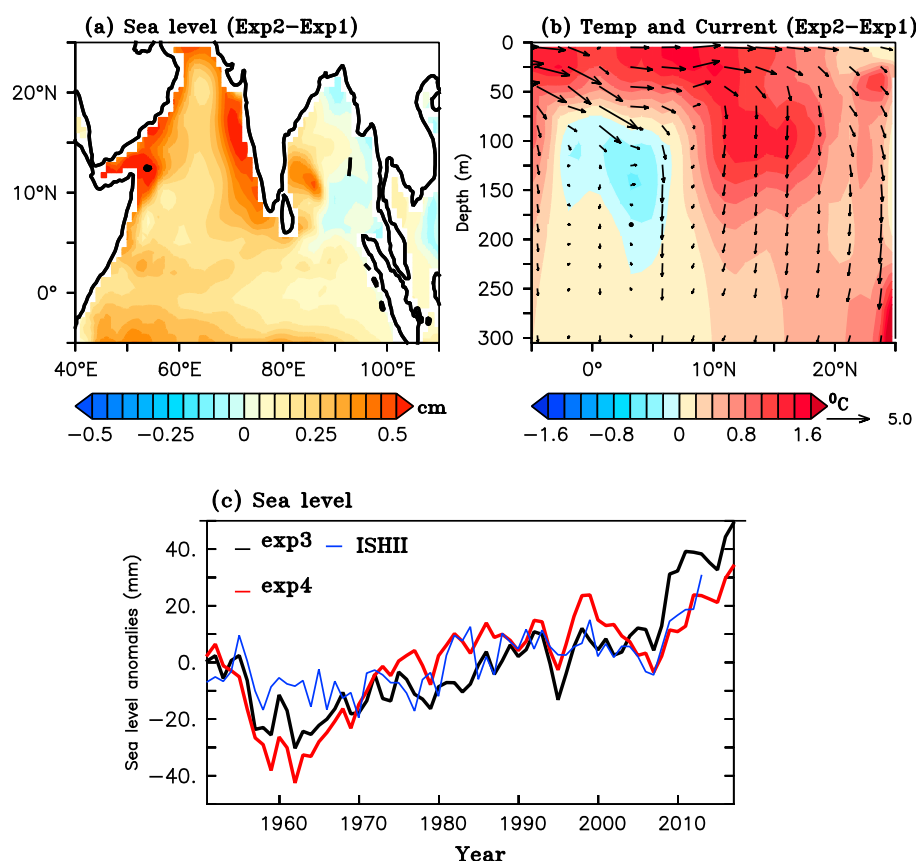


**Figure 3.** Model response between idealized experiments (exp2-exp1) is shown for (a) thermosteric sea level (cm) and (b) subsurface temperature ( $^{\circ}\text{C}$ , shaded) and Indian Ocean cross-equatorial cell represented by meridional and vertical velocity (m/s, vector). (c) Time series of sea level anomalies (mm) in the northern Indian Ocean ( $50^{\circ}$ – $110^{\circ}\text{E}$ ,  $5^{\circ}\text{S}$ – $25^{\circ}\text{N}$ ) from ocean model experiments forced with interannually varying winds.

compared to exp1. The anomalous northward heat transport implies the weakening of southward meridional heat transport in the Indian Ocean.

The anomalously weaker southward heat transport results in warming of subsurface temperatures in the North Indian Ocean as shown by the subsurface temperature difference (shaded) in Figure 3b. The weaker southward meridional heat transport due to a weak cross-equatorial cell results in the accumulation of heat in the North Indian Ocean. Correspondingly, there is an increase in temperature of the water column as shown by the positive subsurface temperature in exp2 as compared to exp1 (Figure 3b). These results are consistent with Thompson et al. (2016), who discuss the decadal-scale spin-down of cross-equatorial cell in response to anomalous winds. Our analysis indicates that the weakening of summer monsoon winds has weakened the southward ocean heat transport and resulted in the weakening of cross-equatorial cell and associated rise in sea level in the North Indian Ocean, especially in the Arabian Sea.

Additionally, to understand the response of multidecadal wind forcing on sea level in the Indian Ocean, we performed OGCM experiments (exp3 and exp4) by forcing the ocean model with interannually varying winds from NCEP reanalysis, keeping all other forcing to climatology. Wind forcing is varied throughout the year in exp3 yet only during May–September (representing summer monsoon wind forcing) in exp4. The climatological winds are used for the remaining months in exp4. The simulation is carried out for the period 1950–2016. The anomalies of sea level in the North Indian Ocean from the experiments are shown in Figure 3c. The anomalies from exp3 (black curve) and exp4 (red curve) show a gradual increase in sea level after the 1970s similar to the thermosteric sea level rise from the Ishii data. The maximum contribution of sea level variability during 1950–2016 (exp3) arises from the summer monsoon as shown by exp4, indicating the dominant role of summer monsoon winds on sea level in the North Indian Ocean. The experiment demonstrates the role of summer monsoon wind forcing on multidecadal sea level variations, with negligible contribution from net heat flux changes in the North Indian Ocean.

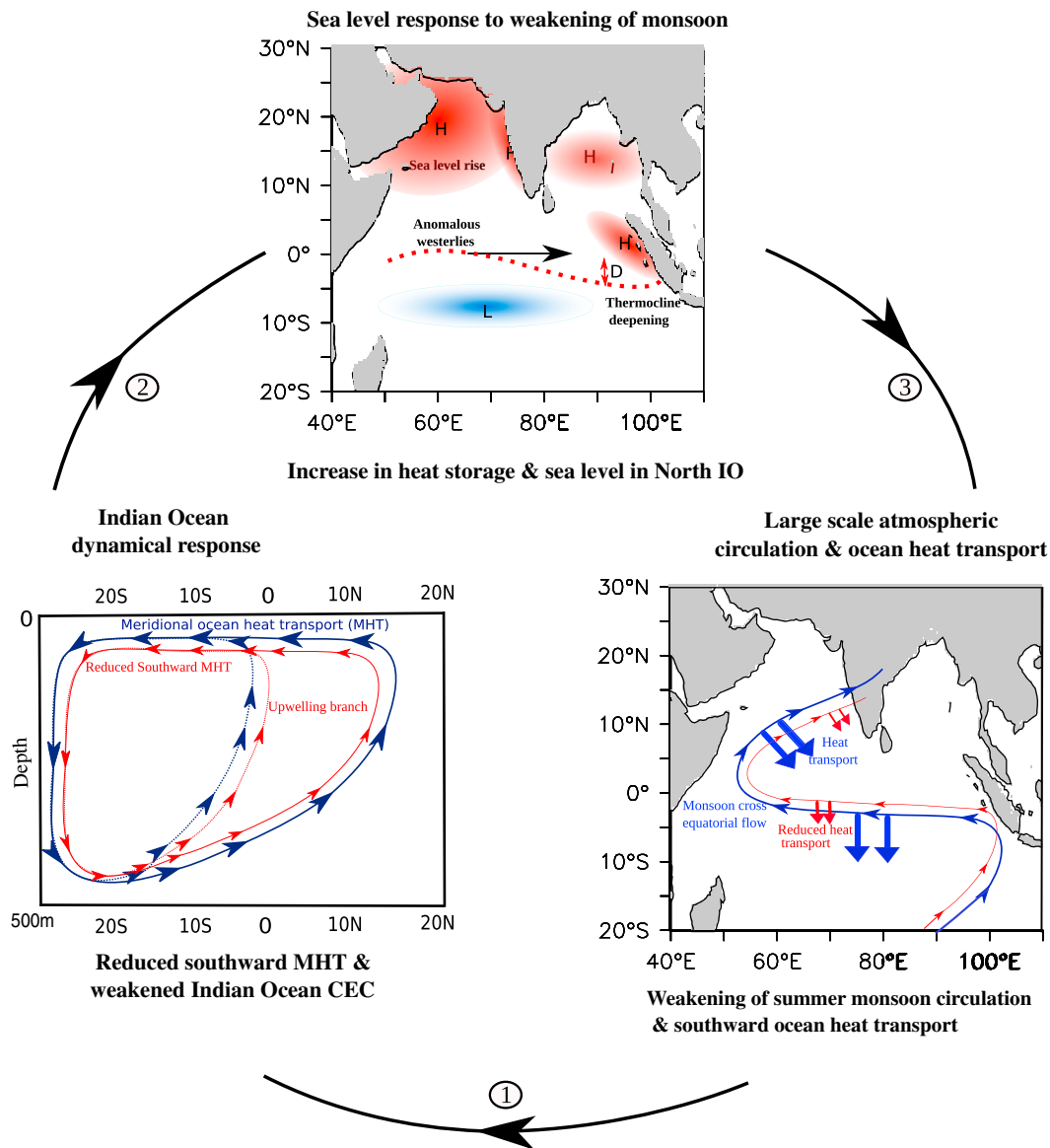


**Figure 4.** Schematic diagram showing sea level response in the North Indian Ocean to multidecadal-scale weakening of summer monsoon circulation. Blue represents climatology, and red represents weakened circulation and weakened southward ocean heat transport. Step 1: weakening of summer monsoon circulation and associated reduction in southward ocean heat transport (red arrows). Step 2: decreased southward meridional heat transport weakens the Indian Ocean cross-equatorial cell. Step 3: weakened cross-equatorial cell with reduced southward meridional heat transport increases heat storage and rise in sea level in the North Indian Ocean. The thermocline deepening associated with sea level rise in the eastern equatorial Indian Ocean enhances equatorial westerlies and weakens the monsoon circulation. The regions of heat gain and sea level rise are marked by H.

### 3.3.3. Synthesis

We estimate the heat storage in the North Indian Ocean from the idealized simulations (exp1 and exp2). Ocean heat storage is calculated as the difference between the net surface heat flux and meridional heat transport. The annual mean southward ocean heat transport is 2.35 PW and 0.5 PW in exp1 and exp2, respectively. In order to focus on the impact from wind changes, the net surface heat flux is kept the same ( $6.53 \text{ W m}^{-2}$ ) for both experiments. The heat storage in the North Indian Ocean in exp2 is higher (6.03 PW) than exp1 (4.07 PW). The heat storage estimate indicates a net storage of heat in the North Indian Ocean when the monsoon circulation is weak, whereas there is a reduction in heat storage during strong monsoon periods. The model results are comparable to the observed changes in heat transport with respect to wind changes.

The heat transport from the northern to southern Indian Ocean has decreased in the recent decades as seen from the meridional volume transport time series in Figure 2d. The reduced volume transport results in the accumulation of heat in the North Indian Ocean after the 1970s. The heat storage estimate from the model experiments also indicates enhanced North Indian Ocean heat storage when the monsoon circulation is weak and vice versa. This mechanism for heat transport change is consistent with Schott and McCreary (2001), who show that Indian Ocean meridional heat transport is dominated by the summer monsoon circulation on interannual time scale. Our analysis reveals multidecadal weakening of summer monsoon circulation and associated reduction in southward heat transport.

In summary, weakening of the monsoon circulation results in weaker southward ocean heat transport and enhanced accumulation of heat in the North Indian Ocean, which in turn increases the thermosteric sea level in the North Indian Ocean, especially in the Arabian Sea, while other mechanism also may contribute to sea level rise in the Bay of Bengal and Sumatra coast. The anomalous westerly winds associated with weakened summer monsoon circulation result in thermocline deepening and sea level rise in the eastern equatorial Indian Ocean. This mechanism is synthesized in the schematic shown in Figure 4.

#### 4. Conclusions and Implications

Sea level in the North Indian Ocean, north of 5°S, has shown considerable increase during recent three to four decades (Figures 1a and 1b). The North Indian Ocean sea level shows multidecadal variability relative to global mean. The thermosteric sea level rise in the North Indian Ocean is estimated to be about  $0.68 \pm 0.03$  mm/yr during 1958–2015 and has accelerated to  $2.3 \pm 0.09$  mm/yr during 1993–2015. Previous studies on Indian Ocean sea level have addressed either the temporal variability of sea level at selected locations or the spatial variability for the recent satellite era (post-1993). However, mechanisms for multidecadal sea level variability are not known.

In the present study, we used long-term tide gauge records and subsurface temperature data to arrive at a mechanistic hypothesis for the regional multidecadal-scale sea level variability in the North Indian Ocean relative to the global mean. Namely, our results connect the observed multidecadal time scale rise in North Indian Ocean sea level to a weakening of summer monsoon circulation during recent three to four decades. Indian Ocean meridional heat transport is dominated by the summer monsoon circulation, with cross-equatorial transport associated with wind-forced Ekman transport (Schott & McCreary, 2001). A weakening monsoon circulation has resulted in reduced southward ocean heat transport and a consequent increase in the North Indian Ocean heat storage. The increased heat storage has thus increased the thermosteric sea level in the North Indian Ocean, especially in the Arabian Sea.

The findings from the study reveal a mechanistic relation between a weakening summer monsoon circulation and sea level rise in the North Indian Ocean. Furthermore, since sea level rise in the North Indian Ocean over the last few decades is close to the global mean sea level rise trend over the same period, it is conceivable that external forcing, other than greenhouse gases (GHG), might have influenced the regional sea level rise via changes in the summer monsoon circulation. For example, it has been suggested that the radiative effects of aerosols (natural and anthropogenic) can be a possible mechanism for offsetting the GHG warming on regional scales (Krishnan & Ramanathan, 2002; Levitus et al., 2005; Ramanathan et al., 2001). Measurements from the Indian Ocean Experiment showed that scattering and absorption of solar radiation by aerosols (e.g., dust, sulfate, black carbon, and organic carbon) over the North Indian Ocean decreases surface solar radiation by more than  $10 \text{ W m}^{-2}$ , leading to reduced evaporation and slowing of the hydrological cycle (Ramanathan et al., 2001). Furthermore, several modeling studies suggest that the radiative effects of increasing anthropogenic aerosol emissions over Asia and Northern Hemisphere have significantly weakened the Indian monsoon circulation and rainfall during the last few decades (Bollasina et al., 2011; Krishnan et al., 2016; Ramanathan et al., 2005). It is also recognized that ocean circulation and sea level variations in a changing climate can be modulated by changes in global water cycle. Clearly, there is a major need for enhancing the present observational and modeling capabilities to better quantify the processes associated with regional sea level variability. The novelty of the present study is the identification of the role of monsoon wind forcing in modulating the regional multidecadal sea level variability in the North Indian Ocean relative to the global mean.

## Acknowledgments

The authors thank IITM for providing support to carry out this research. S. M. G. thanks NOAA/GFDL, the ICTP, Trieste, Italy, and the IITM for supporting a visit to Pune, India, in July 2016 that facilitated his participation in this research. We thank the Editor, Janet Sprintall, and anonymous Reviewers for their valuable suggestions. We also thank Jianjun Yin and Roxy Mathew for their comments on an early draft of this manuscript. All the data sets used for this study are publically available and are described in section 2. The OGCM simulations were performed on the High-Performance Computing System at IITM, Pune.

## References

- Balmaseda, M. A., Mogensen, K., & Weaver, A. T. (2013). Evaluation of the ECMWF ocean reanalysis system ORAS4. *Quarterly Journal of the Royal Meteorological Society*, 139(674), 1132–1161. <https://doi.org/10.1002/qj.2063>
- Berrisford, P., Dee, D., Poli, P., Brugge, R., Fielding, K., Fuentes, M., ... Simmons, A. (2011). The ERA-interim archive version 2.0, ERA report series no. 1. In *European Centre for Medium-Range Weather Forecasts* (23 pp.). UK: Reading.
- Bindoff, N. L., Willebrand, J., Cazenave, A., Gregory, J., Gulev, S., Hanawa, K., ... Unnikrishnan, A. (2007). Observations: Oceanic climate change and sea level. In *Climate Change 2007: The Physical Science Basis. Contribution of Working Group I to the Fourth Assessment Report of the Intergovernmental Panel on Climate Change* (pp. 386–432). Cambridge, UK and York: Cambridge University Press.
- Bollasina, M. A., Ming, Y., & Ramaswamy, V. (2011). Anthropogenic aerosols and the weakening of the South Asian summer monsoon. *Science*, 334, 502–505. <https://doi.org/10.1126/science.1204994>
- Carton, J. A., Giese, B. S., & Grodsky, S. A. (2005). Sea level rise and the warming of the oceans in the Simple Ocean Data Assimilation (SODA) ocean reanalysis. *Journal of Geophysical Research*, 110, C09006. <https://doi.org/10.1029/2004JC002817>
- Chirokova, G., & Webster, P. (2006). Interannual variability of Indian Ocean heat transport. *Journal of Climate*, 19, 1013–1031. <https://doi.org/10.1175/JCLI3676.1>
- Church, J. A., & White, N. J. (2011). Sea-level rise from the late 19th to the early 21st century. *Surveys in Geophysics*, 32(4–5), 585–602. <https://doi.org/10.1007/s10712-011-9119-1>
- Church, J. A., White, N. J., Konikow, L. F., Domingues, C. M., Graham Cogley, J., Rignot, E., ... Velicogna, I. (2013). Erratum: Revisiting the Earth's sea-level and energy budgets from 1961 to 2008. *Geophysical Research Letters*, 40, 4066. <https://doi.org/10.1002/grl.50752>
- Dee, D. P., Uppala, S. M., Simmons, A. J., Berrisford, P., Poli, P., Kobayashi, S., ... Vitart, F. (2011). The ERA-Interim reanalysis: Configuration and performance of the data assimilation system. *Quarterly Journal of the Royal Meteorological Society*, 137(656), 553–597. <https://doi.org/10.1002/qj.828>
- Gill, A. E. (1980). Some simple solutions for heat-induced tropical circulation, East. *Quarterly Journal of the Royal Meteorological Society*, 106, 447–462.
- Good, S. A., Martin, M. J., & Rayner, N. A. (2013). EN4: Quality controlled ocean temperature and salinity profiles and monthly objective analyses with uncertainty estimates. *Journal of Geophysical Research: Oceans*, 118, 6704–6716. <https://doi.org/10.1002/2013JC009067>
- Griffies, S. M., Biastoch, A., Böning, C., Bryan, F., Danabasoglu, G., Chassignet, E. P., ... Yin, J. (2009). Coordinated Ocean-ice Reference Experiments (COREs). *Ocean Modelling*, 26(1–2), 1–46. <https://doi.org/10.1016/j.ocemod.2008.08.007>
- Griffies, S. M., Yin, J., Durack, P. J., Goddard, P., Bates, S. C., Behrens, E., ... Zhang, X. (2014). An assessment of global and regional sea level for years 1993–2007 in a suite of interannual core-II simulations. *Ocean Modelling*, 78, 35–89. <https://doi.org/10.1016/j.ocemod.2014.03.004>
- Han, W., Meehl, G. A., Rajagopalan, B., Fasullo, J. T., Hu, A., Lin, J., ... Yeager, S. (2010). Patterns of Indian Ocean sea-level change in a warming climate. *Nature Geoscience*, 3(8), 546–550. <https://doi.org/10.1038/ngeo901>
- Han, W., Vialard, J., McPhaden, M. J., Lee, T., Masumoto, Y., Feng, M., & De Ruijter, W. P. M. (2014). Indian Ocean decadal variability: A review. *Bulletin of the American Meteorological Society*, 95(11), 1679–1703. <https://doi.org/10.1175/BAMS-D-13-00028.1>
- Ishii, M., Kimoto, M., & Kachi, M. (2003). Historical ocean subsurface temperature analysis with error estimates. *Monthly Weather Review*, 131(1), 51–73. [https://doi.org/10.1175/1520-0493\(2003\)131%3C0051:HOSTAW%3E2.0.CO;2/cie](https://doi.org/10.1175/1520-0493(2003)131%3C0051:HOSTAW%3E2.0.CO;2/cie)
- Jadhav, J., Panickal, S., Marathe, S., & Ashok, K. (2015). On the possible cause of distinct El Niño types in the recent decades. *Scientific Reports*. <https://doi.org/10.1038/srep17009>
- Kendall, M. G. (1975). *Rank Correlation Methods* (4th ed.). Charles Griffin: London.
- Kistler, R., Collins, W., Saha, S., White, G., Woollen, J., Kalnay, E., ... Fiorino, M. (2001). The NCEP-NCAR 50-year reanalysis: Monthly means CD-ROM and documentation. *Bulletin of the American Meteorological Society*, 82(2), 247–267. [https://doi.org/10.1175/1520-0477\(2001\)082%3C0247:TNNYRM%3E2.3.CO;2](https://doi.org/10.1175/1520-0477(2001)082%3C0247:TNNYRM%3E2.3.CO;2)
- Kobayashi, S., Ota, Y., Harada, Y., Ebata, A., Moriwa, M., Onoda, H., ... Takahashi, K. (2015). The JRA-55 reanalysis: General specifications and basic characteristics. *Journal of the Meteorological Society of Japan. Series II*, 93(1), 5–48. <https://doi.org/10.2151/jmsj.2015-001>
- Krishnamurti, T. N., & Bhalme, H. N. (1976). Oscillations of a monsoon system. Part I. Observational aspects. *Journal of the Atmospheric Sciences*, 33, 1937–1954. [https://doi.org/10.1175/1520-0469\(1976\)033%3C1937:OAMSP%3E2.0.CO;2](https://doi.org/10.1175/1520-0469(1976)033%3C1937:OAMSP%3E2.0.CO;2)
- Krishnan, R., & Ramanathan, V. (2002). Evidence for surface cooling from absorbing aerosols. *Geophysical Research Letters*, 29(54), 1340. <https://doi.org/10.1029/2002GL014687>
- Krishnan, R., & Swapna, P. (2009). Significant influence of the boreal summer monsoon flow on the Indian Ocean response during dipole events. *Journal of Climate*, 22(21), 5611–5634. <https://doi.org/10.1175/2009JCLI2176.1>
- Krishnan, R., Ramesh, K. V., Samala, B. K., Meyers, G., Slingo, J. M., & Fennessy, M. J. (2006). Indian Ocean-monsoon coupled interactions and impending monsoon droughts. *Geophysical Research Letters*, 33, L08711. <https://doi.org/10.1029/2006GL025811>
- Krishnan, R., Sabin, T. P., Vellore, R., Mujumdar, M., Sanjay, J., Goswami, B. N., ... Terray, P. (2016). Deciphering the desiccation trend of the South Asian monsoon hydroclimate in a warming world. *Climate Dynamics*, 47(3–4), 1007–1027. <https://doi.org/10.1007/s00382-015-2886-5>
- Large, W. G., & Yeager, S. G. (2009). The global climatology of an interannually varying air-sea flux dataset. *Climate Dynamics*, 33, 341–361. <https://doi.org/10.1007/s00382-008-0441-3>
- Lee, T., & McPhaden, M. J. (2008). Decadal phase change in large-scale sea level and winds in the Indo-Pacific region at the end of the 20th century. *Geophysical Research Letters*, 35, L01605. <https://doi.org/10.1029/2007GL032419>
- Levitus, S., Antonov, J., & Boyer, T. (2005). Warming of the world ocean, 1955–2003. *Geophysical Research Letters*, 32, L02604. <https://doi.org/10.1029/2004GL021592>
- Levitus, S., Antonov, J. I., Boyer, T. P., Baranova, O. K., Garcia, H. E., Locarnini, R. A., ... Zweng, M. M. (2012). World ocean heat content and thermocline sea level change (0–2000 m), 1955–2010. *Geophysical Research Letters*, 39, L10603. <https://doi.org/10.1029/2012GL051106>
- Li, Y., & Han, W. (2015). Decadal sea level variations in the Indian Ocean investigated with HYCOM: Roles of climate modes, ocean internal variability, and stochastic wind Forcing. *Journal of Climate*, 28, 9143–9165. <https://doi.org/10.1175/JCLI-D-15-0252.1>
- Liu, X., Köhl, A., & Stammer, D. (2017). Dynamical ocean response to projected changes of the global water cycle. *Journal of Geophysical Research: Oceans*, 122, 6512–6532. <https://doi.org/10.1002/2017JC013061>
- Loschnigg, J., & Webster, P. J. (2000). A coupled ocean–Atmosphere system of SST modulation for the Indian Ocean. *Journal of Climate*, 13, 3342–3360. [https://doi.org/10.1175/1520-0442\(2000\)013%3C3342:ACOASO%3E2.0.CO;2](https://doi.org/10.1175/1520-0442(2000)013%3C3342:ACOASO%3E2.0.CO;2)
- Mann, H. B. (1945). Nonparametric test against trend. *Econometrica*, 13, 245–259.
- Miyama, T., McCreary, J. P., Jensen, T. G., Loschnigg, J., Godfrey, S., & Ishida, A. (2003). Structure and dynamics of the Indian-Ocean cross-equatorial cell. *Deep Sea Research Part II: Topical Studies in Oceanography*, 50(12–13), 2023–2047. [https://doi.org/10.1016/S0967-0645\(03\)00044-4](https://doi.org/10.1016/S0967-0645(03)00044-4)

- Narayanasetti, S., Swapna, P., Ashok, K., Jadhav, J., & Krishnan, R. (2016). Changes in biological productivity associated with Ningaloo Niño/Niña events in the southern subtropical Indian Ocean in recent decades. *Scientific Reports*, 1–8. <https://doi.org/10.1038/srep27467>
- Neil, W. J., Haigh, I. D., Church, J. A., Koen, T., Christopher, S. W., Pritchard, T. R., ... Tregoning, P. (2014). Australian sea levels—Trends, regional variability and influencing factors. *Earth-Science Reviews*, 136, 155–174. <https://doi.org/10.1016/j.earscirev.2014.05.011>
- Nidheesh, A. G., Lengaigne, M., Vialard, J., Unnikrishnan, A. S., & Dayan, H. (2013). Decadal and long-term sea level variability in the tropical Indo-Pacific Ocean. *Climate Dynamics*, 41(2), 381–402. <https://doi.org/10.1007/s00382-012-1463-4>
- North, G. R., Bell, T. L., Cahalan, R. F., & Moeng, F. J. (1982). Sampling errors in the estimation of empirical orthogonal functions. *Monthly Weather Review*, 110(699–706). [https://doi.org/10.1175/1520-0493\(1982\)110%3C0699:SEITEO%3E2.0.CO;2](https://doi.org/10.1175/1520-0493(1982)110%3C0699:SEITEO%3E2.0.CO;2)
- Parekh, A., Gnanaseelan, C., Deepa, J. S., Karmakar, A., & Chowdary, J. S. (2017). In R. Rajeevan, & S. Naik (Eds.), *Sea Level Variability and Trends in the North Indian Ocean: Observed Climate Variability and Change Over the Indian Region* (pp. 181–192). Singapore: Springer.
- Ramanathan, V., Chung, C., Kim, D., Bettge, T., Buja, L., Kiehl, J. T., ... Wild, M. (2005). Atmospheric brown clouds: Impacts on South Asian climate and hydrological cycle. *Proceedings of the National Academy of Sciences of the United States of America*, 102(15), 5326–5333. <https://doi.org/10.1073/pnas.0500656102>
- Ramanathan, V., Crutzen, P. J., Lelieveld, J., Mitra, A. P., Althausen, D., Anderson, J., ... Valero, F. P. J. (2001). Indian Ocean experiment: An integrated analysis of the climate forcing and effects of the great Indo-Asian haze. *Journal of Geophysical Research*, 106, 28,371–28,398. <https://doi.org/10.1029/2001JD900133>
- Ramesh Kumar, M. R., Krishnan, R., Syam, S., Unnikrishnan, A. S., & Pai, D. S. (2009). Increasing trend of “Break-Monsoon” conditions over India —Role of ocean-atmosphere processes in the Indian Ocean. *IEEE Geoscience and Remote Sensing Letters*, 6, 332–336.
- Rhein, M., Rintoul, S. R., Aoki, S., Campos, E., Chambers, D., Feely, R. A., ... Wang, F. (2013). *Chapter 3: Observations: Ocean, Fifth Assessment Report of the Intergovernmental Panel on Climate Change*. Cambridge, UK and New York: Cambridge University Press.
- Rodwell, M. J. (1997). Breaks in the Asian monsoon: The influence of Southern Hemisphere weather systems. *Journal of the Atmospheric Sciences*, 54(22), 2597–2611. [https://doi.org/10.1175/1520-0469\(1997\)054%3C2597:BITAMT%3E2.0.CO;2](https://doi.org/10.1175/1520-0469(1997)054%3C2597:BITAMT%3E2.0.CO;2)
- Salim, M., Nayak, R. K., Swain, D., & Dadhwal, V. K. (2012). Sea surface height variability in the tropical Indian Ocean: Steric contribution. *Journal of the Indian Society of Remote Sensing*, 40(4), 679–688. <https://doi.org/10.1007/s12524-011-0188-x>
- Schoenefeldt, R., & Schott, F. A. (2006). Decadal variability of the Indian Ocean cross-equatorial exchange in SODA. *Geophysical Research Letters*, 33, L08602. <https://doi.org/10.1029/2006GL025891>
- Schott, F. A., & McCreary, J. P. (2001). The monsoon circulation of the Indian Ocean. *Progress in Oceanography*, 51(1), 1–123. [https://doi.org/10.1016/S0079-6611\(01\)00083-0](https://doi.org/10.1016/S0079-6611(01)00083-0)
- Schott, F. A., Xie, S.-P., & McCreary, J. P. Jr. (2009). Indian Ocean circulation and climate variability. *Reviews of Geophysics*, 47, RG1002. <https://doi.org/10.1029/2007RG000245>
- Schwarzkopf, F. U., & Böning, C. W. (2011). Contribution of Pacific wind stress to multi-decadal variations in upper-ocean heat content and sea level in the tropical south Indian Ocean. *Geophysical Research Letters*, 38, L12602. <https://doi.org/10.1029/2011GL047651>
- Stammer, D., Cazanave, A., Ponte, R. M., & Tamisiea, M. E. (2013). Causes for contemporary regional sea level changes. *Annual Review of Marine Science*, 5, 21–46. <https://doi.org/10.1146/annurev-marine-121211-172406>
- Swapna, P., Krishnan, R., & Wallace, J. M. (2014). Indian Ocean and monsoon coupled interactions in a warming environment. *Climate Dynamics*, 42(9–10), 2439–2454. <https://doi.org/10.1007/s00382-013-1787-8>
- Thompson, P. R., Piecuch, C. G., Merrifield, M. A., McCreary, J. P., & Firing, E. (2016). Forcing of recent decadal variability in the Equatorial and North Indian Ocean. *Journal of Geophysical Research: Oceans*, 121, 6762–6778. <https://doi.org/10.1002/2016JC012132>
- Trenary, L. L., & Han, W. (2013). Local and remote forcing of decadal sea level and thermocline depth variability in the South Indian Ocean. *Journal of Geophysical Research: Oceans*, 118, 381–398. <https://doi.org/10.1029/2012JC008317>
- Unnikrishnan, A. S., & Shankar, D. (2007). Are sea-level-rise trends along the coasts of the North Indian Ocean consistent with global estimates? *Global and Planetary Change*, 57(3–4), 301–307. <https://doi.org/10.1016/j.gloplacha.2006.11.029>
- Unnikrishnan, A. S., Sundar, D., Blackman, D., Kumar, K. R., & Michael, G. S. (2006). Sea level changes along the coast of India: Observations and projections. *Current Science*, 90(3), 362–368.
- Webster, P. J., & Yang, S. (1992). Monsoon and ENSO: Selectively interactive systems. *Quarterly Journal of Royal Meteorological Society*, 118, 877–926.
- Woodworth, P. L., & Player, R. (2003). The permanent service for mean sea level: An update to the 21st century. *Journal of Coastal Research*, 19, 287–295.